PHYSICAL REVIEW B VOLUME 40, NUMBER 8 15 SEPTEMBER 1989-I

Chemical and electronic properties of the Ag/GaSb(110) interface formed at room and low temperature

D. Mao and A. Kahn
Department of Electrical Engineering, Princeton University, Princeton, New Jersey 08544-5263

L. Soonckindt
Laboratoire d'Etudes des Surfaces, Interfaces et Composants, Université des Sciences et Techniques du Languedoc, place Eugène Bataillon, 34060 Montpellier CEDEX, France
(Received 1 May 1989)

Ultraviolet photoemission spectroscopy, electron-energy-loss spectroscopy, Auger-electron spectroscopy, and x-ray photoemission spectroscopy were used to study the formation of Ag/GaSb(110) interfaces at room and low temperature. Interfaces formed at room temperature show extensive Ag clustering and some chemical redistribution due to interface disruption. A substantial reduction in adatom surface mobility and clustering is observed at low temperature. The resulting changes in surface Fermi-level (E_F) movements, namely the overshoot of the E_F position on *p*-type samples and the delayed E_F movement on *n*-type samples, confirm earlier trends found on low-temperature GaAs. E_F pinning is found to occur in a coverage range where metallicity appears in the overlayer.

I. INTRODUCTION

In order to discriminate experimentally between the various Schottky-barrier models put forth during the past decade, studies of interfaces formed on (110) vacuum-cleaved low-temperature (LT 80 K) GaAs have recently been performed.[1–9] The goal for these LT depositions was to measure the impact of a reduction in adatom clustering and interface reaction on the Fermi-level (E_F) -pinning process, thereby allowing an easier identification of the dominant pinning mechanisms. It was found that the LT band bending as a function of metal coverage was altered in a similar fashion at all the interfaces investigated. Quasisymmetric movements toward midgap are generally observed on room-temperature (RT) *n*- and *p*-type GaAs. At LT the low-coverage E_F movements are highly asymmetric: rapid movement up in the gap on *p*-type GaAs with less than 0.1 monolayer (ML), and overshoot above the final pinning position; very little movement down in the gap on *n*-type GaAs up to 1–2 ML of metal, followed by a rapid transition to the near-midgap pinning position.

This LT behavior was explained with the formation of donorlike states induced by the bonding of isolated adatoms to the substrate.[10–12] These states affect band bending only on *p*-type substrates and cause the rapid rise of E_F. The energy level of these states was found to correlate with the ionization energy of the adatom.[10–12] The adsorption of the metal atom also induces acceptor states that are near or above the conduction-band minimum and, as such, minimally affect band bending on *n*-type substrates. Klepeis *et al.*[13] recently calculated that the energy gap between the donor and acceptor levels is of the order of 1 eV. The exact position of these levels and their energy difference depend, however, on the geometrical details of the adsorption, which are still mostly unknown. Lefebvre *et al.*[14] and Klepeis *et al.*[13] also calculated that, as the metal coverage increases, the adatom-substrate dipoles shift these levels up or down depending on the sign of the adatom-substrate charge transfer (toward the valence band in the case of a weakly electronegative adatom). At higher coverage the proximity of these dipoles leads to a depolarization of the adatom-substrate bonds, and to the saturation of the shift. The overlap between wave functions of neighbor adatoms becomes nonnegligible and broadens the adsorbate-induced states. E_F moves down from the overshoot position on *p*-type samples and is forced down from the conduction band by the shifted and broadened acceptor band on *n*-type samples. We also note that the completion of band bending at the semiconductor surface has been correlated for several interfaces with the onset of metallic character on the overlayer, as seen from the appearance of a substantial density of states at the Fermi level or from the broadening of the *d* band in Au or Ag with photoemission spectroscopy.[3,15–18] The principal achievement of these LT studies was therefore to slow down adatom clustering and retard the onset of metallicity in the overlayer, so that this sequence of events could be unraveled. Recent studies of metal deposition on RT and LT InP have also invoked the competition between defects and metal-induced gap states (MIG's) in the pinning process.[19] A major step forward made during the past year was perhaps to realize that both types of mechanisms may coexist with relative strengths that depend on the specific interface and on the conditions of interface formation.

Interfaces between metals and several other compound semiconductors should be investigated before full credibility can be given to these concepts. The suggestion that deep-level bulk defects present in liquid-encapsulated Czochralski (LEC) -grown GaAs might play a role in the E_F pinning has underscored the importance of investigat-

 ©1989 The American Physical Society

ing other semiconductor materials.[20] We present here results concerning the Ag/GaSb(110) interface. GaSb interfaces have received little attention in the past decade, although the 0.72-eV gap of this semiconductor makes it interesting for multiple applications in communication and detection. GaSb has a small heat of formation (10 kcal/mol) and thus is susceptible to strong interface disruption upon metal deposition. This has been observed with Au/GaSb (Ref. 21) and Ag/GaSb (Ref. 22). The study of interfaces formed at LT should therefore be very informative on the role of defects or other mechanisms in the formation of the barrier. Our study involves measurements of band bending with ultraviolet photoemission spectroscopy (UPS), and of interface reaction, chemical composition, and morphology with Auger-electron spectroscopy (AES), x-ray photoemission spectroscopy (XPS), and electron-energy-loss spectroscopy (EELS). The results are consistent with the general picture obtained with other metals as well as Ag on GaAs (Refs. 2, 12, and 15): Ag grows in three-dimensional clusters on RT GaSb (Volmer-Weber growth mode); deposition at LT reduces surface mobility and clustering of Ag; the low-coverage movement of E_F is different from the RT case, and consistent with an adsorbate-induced–gap-state model; final pinning of E_F is delayed with respect to the RT case, and correlates with the onset of metallic character in the overlayer; the final E_F-pinning position is compatible with the charge-neutrality-level position calculated by Tersoff.[23]

II. EXPERIMENTS

Measurements were performed on GaSb samples cleaved in ultrahigh vacuum (10^{-10} Torr). Highly doped (Te, $n=1.1\times10^{+18}$ cm^{-3}; Zn, $p=2.8\times10^{+18}$ cm^{-3}) and moderately doped (Te, $n=2.2\times10^{+17}$ cm^{-3}; Zn, $p=1.8\times10^{+17}$ cm^{-3}) samples were used. Ohmic contacts were made by evaporating Au on p-type GaSb and (Au,Sn) on n-type GaSb under vacuum conditions and annealing at 260 °C in a mixed hydrogen-nitrogen ambient. Cleaving, metal deposition, and measurements were done at RT or LT (35 K). The evaporation of Ag was done from a W basket at typical rates of 1 ML/min. For GaSb, 1 ML represents $0.76\times10^{+15}$ atoms/cm^2 and has a nominal thickness of 1.3 Å. Depositions of In were also performed to verify the position of the Fermi level of the system. AES measurements were done in the first-derivative mode with a primary–electron-beam energy of 3 keV and a peak-to-peak modulation of 0.5 V. EELS measurements were done in the second-derivative mode with a primary–electron-beam energy of 150 eV and a peak-to-peak modulation of 0.5 V. XPS measurements were done with 151.4-eV photons produced by an x-ray source equipped with a Zr anode. This photon energy gives high surface sensitivity for Ga 3d and Sb 4d core-level measurements. Finally, the UPS measurements were done with a nonmonochromatized He lamp using the He II (40.8-eV) and He III (48.4-eV) lines for the valence band and Ga 3d core level, respectively. The He pressure in the chamber was in the 10^{-9} Torr range during measurement. The electron-energy analyzer for all the techniques mentioned above was a double-pass cylindrical mirror analyzer. The estimated resolution for the UPS measurements was 0.15 eV.

III. RESULTS AND DISCUSSION

A. Overlayer morphology and interface reaction

The overlayer morphology and interface reactivity were evaluated with AES, XPS, and EELS. The Sb $M_4N_{4,5}N_{4,5}$ and Ga $L_3M_{4,5}M_{4,5}$ peaks are shown in Fig. 1 as a function of Ag coverage. The line shape of the Sb peak is conserved up to high coverages, with a slight loss

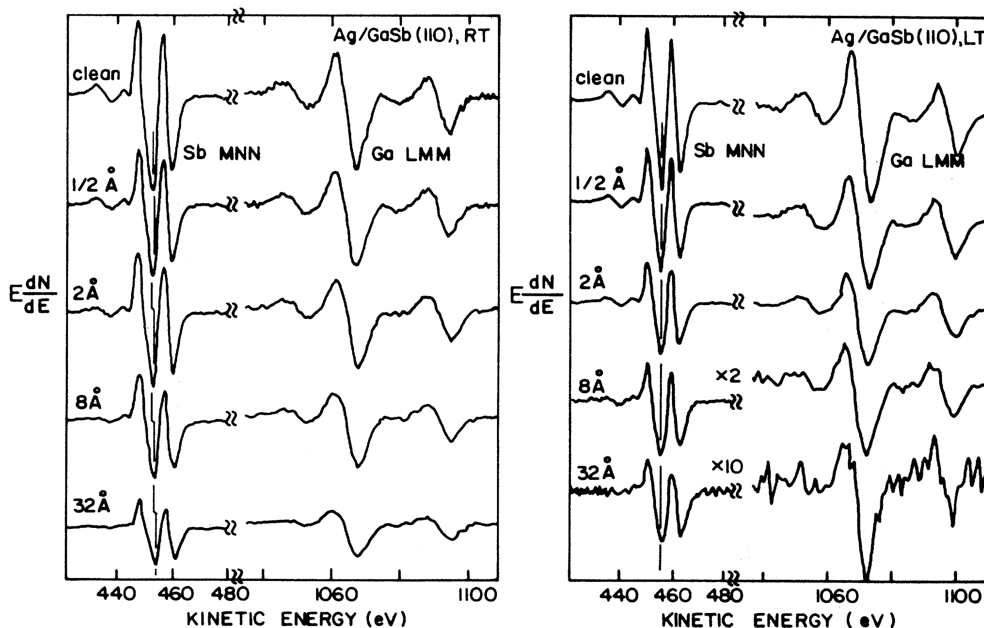

FIG. 1. AES Sb 453-eV and Ga 1068-eV peaks as a function of Ag coverage on the RT and LT GaSb surface.

of resolution above 16 Å at RT and 8 Å at LT. No significant peak broadening is observed. A 1.5-eV shift toward higher energy occurs at RT above 4–8 Å, indicating some disruption of the surface and modification of the chemical environment of Sb. This is in agreement with soft-x-ray photoemission results obtained by Walters *et al.*[22] The XPS measurements also indicate interface disruption. The large Ga-to-Sb peak ratio in Fig. 2 is due to the fact that the 151.4-eV photon energy gives photoemission near the Cooper minimum for the Sb 4*d* core level. Thus, sensitivity to Sb is reduced. The RT data clearly show a perturbation of the Ga peak at high coverage: the peak shifts by 1.5 eV to higher binding energy and its full width at half maximum (FWHM) increases from 1.8 eV on clean GaSb to 3.0 eV with 64 Å Ag. The 1.5-eV shift occurs long after saturation of the band bending (see below) and is attributed to chemical effects. The increase in the FWHM is presumably due to a distribution of nonequivalent Ga species, from Ga in GaSb to Ga diluted in or segregated on top of Ag. High-resolution core-level photoemission experiments[24] show that, at high coverages, the Ga 3*d* peak shifts toward low binding energy. GaSb is disrupted and free Ga is formed. The shift toward high binding energy observed here appears therefore to be a spurious effect due perhaps to contamination.

At LT the Sb AES peak shifts by less than 0.5 eV. Very little shift or broadening is observed in the XPS data below 8 Å, the coverage at which the signal becomes too small to be usable. Interface dissociation appears therefore to be reduced at 35 K, although not completely eliminated. The kinetically limited redistribution of released species also attenuates the "fingerprint" of dissociation in the photoemission spectrum.

The attenuation of the AES Ga and Sb peaks and of the XPS Ga 3*d* peak as a function of Ag coverage is shown in Fig. 3. The relative rates of attenuation at RT and LT agree well with the different electron-escape depths involved in the measurements: 5–6 Å for the 128-eV XPS Ga 3*d* electrons, 8–10 Å for the 453-eV AES Sb electrons, and 15–20 Å for the 1068-eV AES Ga electrons. As expected, the attenuation is more rapid at LT than at RT, where the Volmer-Weber growth leaves significant areas of the GaSb surface uncovered. In addition, the AES Ga and Sb signals are attenuated at the same rate at RT, whereas the Sb signal is attenuated faster at LT. Clustering at RT produces a nonlaminar growth in islands separated by uncovered areas of stoichiometric GaSb. The signal from these bare areas dominates because of the finite electron-escape depth through the Ag islands. Thus, the attenuation of the substrate signal reflects only an increase in the percentage of the surface area covered with thick islands, and is the same for Ga and Sb (Fig. 3). The electron energies of the Ga and Sb AES peaks do not provide sufficient surface sensitivity to pick up the differential rate of diffusion of Ga and Sb through the Ag layer found with soft-x-ray photoemission spectroscopy.

At LT the attenuation results from an increase in the thickness of an homogeneous Ag layer, and the difference between the escape depths of the Sb and Ga Auger electrons through Ag yields the observed difference in the attenuation rates (Fig. 3). The LT high-coverage attenuation rates are comparable to the exponential decay expected for a completely laminar growth. A surprising result is the initial attenuation rate (below 1 Å), which is extremely fast at RT and LT, and corresponds to escape

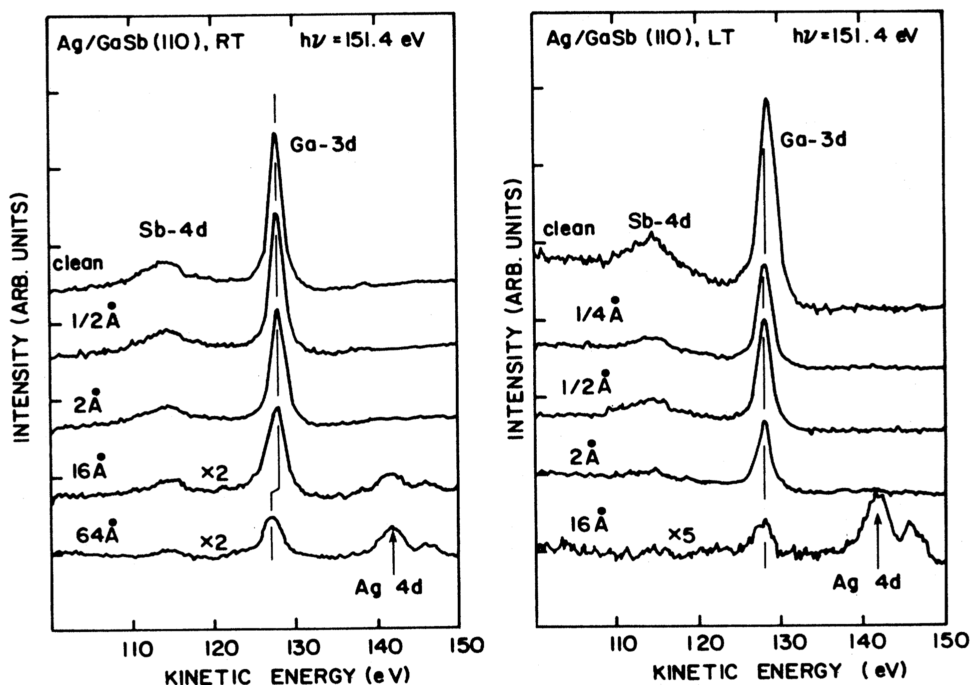

FIG. 2. XPS Sb 4*d* and Ga 3*d* spectra as a function of Ag coverage on the RT and LT GaSb surface. The photon energy is 151 eV.

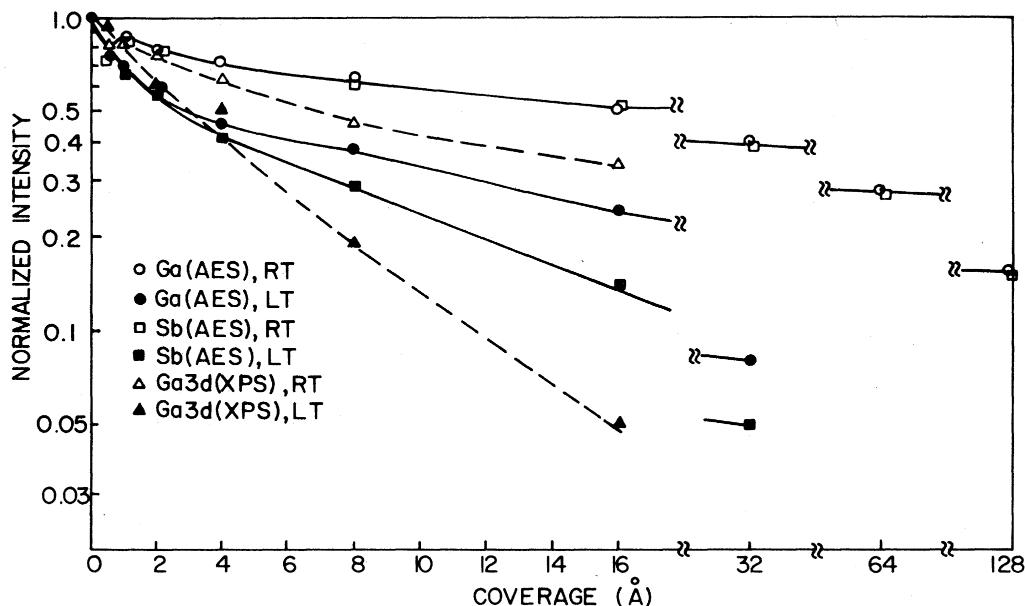

FIG. 3. Attenuation of the normalized intensities of the AES Ga and Sb and XPS Ga peaks as a function of coverage on the RT and LT GaSb surface.

depths of the order of 2 Å. Such short escape depths have been observed before with two-dimensional metal layers.[2] However, we demonstrate below that the RT Ag layer follows a Volmer-Weber growth mode even at submonolayer coverages, and therefore cannot warrant the observed exponential decay. Surface chemical effects or structural changes, on the other hand, could affect the Auger-peak shapes.

B. Electron-energy-loss spectroscopy of the interface

The RT and LT EELS spectra are shown in Fig. 4. The clean GaSb spectra show the features identified by van Laar *et al.*[25]: valence-band–to–conduction-band transitions at 2.8 and 5.4 eV, a surface-plasmon transition at 9.6 eV, a bulk-plasmon transition at 14.8 eV, a surface-exciton transition at 20 eV, Ga 3*d*–to–conduction-band transitions at 21.2 and 23 eV, and a Sb 4*d*–to–conduction-band transition showing the spin-orbit splitting at 33–34 eV. The surface exciton (SE) corresponds to a transition between the Ga 3*d* core level and the empty dangling bond of the Ga atom on the relaxed surface. As it involves a surface state, this transition is very sensitive to the quality of the surface, as well as to any perturbation of the cation dangling bond by an adsorbate.[26] It provides a much more accurate measure of surface effective coverage by the overlayer than does AES or XPS at low coverages.

With RT deposition the magnitude of all the peaks slowly decreases due to the buildup of the Ag layer that screens the substrate from the interaction with the primary electron. Yet, the SE remains clearly visible with 4 Å Ag ($\sim$3 ML). This attenuation rate is incompatible with a Stranski-Krastanov growth mode, which should eliminate the surface features with about 0.5 ML. It reflects a three-dimensional growth and nucleation at very low coverage. The strongest perturbation of the spectrum is between 3 and 9 eV, where the main Ag loss features appear. The Ag bulk plasmon ($\sim$4 eV) dominates the spectrum beyond 8 Å coverage.

With LT deposition the SE and surface-plasmon peaks are attenuated much faster than features corresponding to bulk transitions, indicating a modification of the electronic properties of the entire surface, over and beyond the simple effects of increasing metal thickness. In particular, the SE disappears with only $\sim$0.5 Å Ag ($\leq$0.39 ML), which, given the inaccuracy of the deposition process, corresponds to slightly less than one Ag atom per surface unit cell. We believe that the elimination of the SE at such low coverage is an indication that Ag preferentially adsorbs on the surface Ga. If Ag did adsorb randomly on both surface species at low coverage, one should observe either a slower decrease in the SE strength versus coverage, or a shift of the SE peak toward lower-energy losses. This shift would correspond to a shift of the Ga dangling-bond energy into the gap due to the Ag-induced unrelaxation of the surface. Adatom-induced surface unrelaxation is to be expected because the charge transfer between the surface cation and anion unsaturated dangling bonds partially drives the clean-surface relaxation. Unrelaxation has been observed with Ag,[2] Al,[27] or Sn (Ref. 4) on GaAs, and a preliminary low-energy electron-diffraction (LEED) investigation suggests that it is also the case for Ag/GaSb.[28] Given that the position of the empty Ga dangling bond on the relaxed GaSb surface is about 0.4 eV above the conduction-band minimum,[25] and that the gap is 0.81 eV at 35 K, the shift should be at most 0.7–0.8 eV toward lower-energy loss. This is not observed in the EELS data. We believe therefore that the rapid elimination of the SE peak is best explained by direct bonding between the Ag adatom and the surface Ga. This is supported

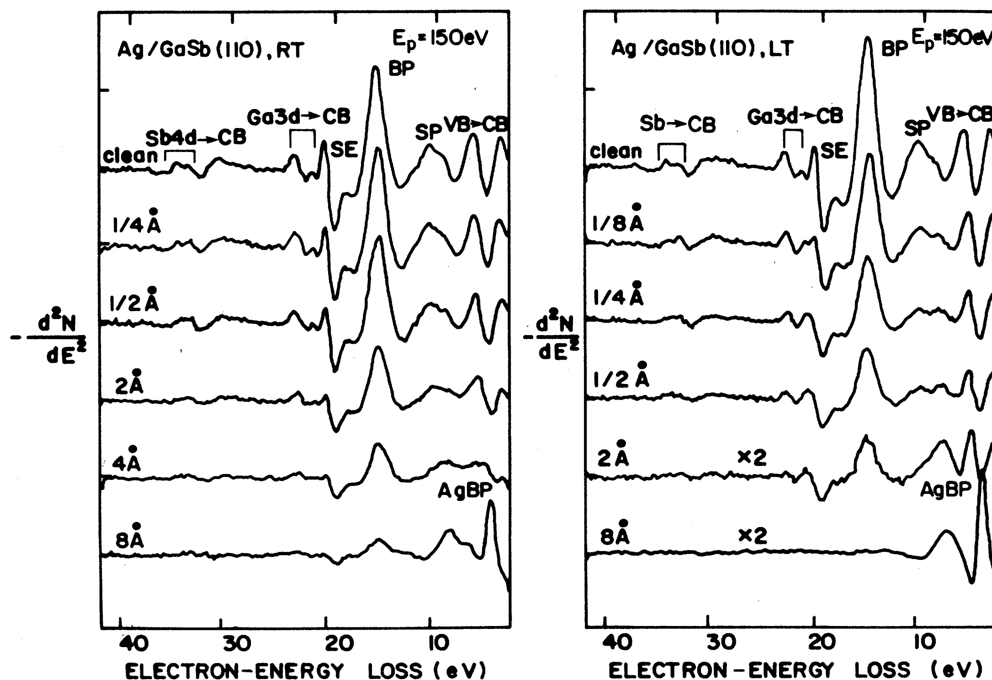

FIG. 4. EELS GaSb spectra as a function of Ag coverage on the RT and LT surface. BP denotes bulk plasmon, SP surface plasmon, SE surface exciton, and VB→CB valence-band–to–conduction-band transition. The primary electron energy is 150 eV.

by a recent scanning-tunneling-microscopy study of Au/GaAs(110), which indicates that Au adatoms occupy the Ga site.[29]

The 8-eV Ag peak also increases more rapidly than at RT. It grows and saturates at high coverage, which shows that it is a Ag-related loss and is unrelated to the Ag-GaSb interaction. It also appears long before the Ag bulk plasmon. Thus we attribute this peak to a more atomiclike loss, such as the transition between the 4*d* level and an empty state in the atom. Its prominence at LT might reflect an excitation cross section larger for adatoms spread in a two-dimensional layer. In conclusion, and regardless of the details of the adsorption geometry, the EELS results complete and confirm for the ultralow-coverage regime (<0.5 ML) the results obtained from AES and XPS at higher coverage. The LT low-coverage Ag layer is two dimensional and presumably composed of isolated adatoms or very small clusters (few adatoms), a result which is crucial for the interpretation of the UPS data.

C. UPS and Fermi-level movements

The valence-band electron-distribution curves (EDC's) measured with 40.8-eV photons as a function of Ag deposition are shown in Fig. 5. The clean-surface EDC's are in good agreement with previously published data.[21] The peak at 12 eV below the valence-band maximum (E_v) corresponds to the Ga 3*d* core level excited by the He III (48.4-eV) line, and is used to measure E_F movements at the GaSb surface.

We focus first on the shape of the low-coverage Ag 4*d* peak, which depends sensitively on the overlayer growth mode (Fig. 5). The peak is characterized by a doublet resulting from the hybridization between the 4*d* and 5*s* levels. At RT this doublet is resolved above 1/8 Å (~0.1 ML). The low-coverage LT peak is more atomiclike and the doublet is resolved only above 2 Å. The solid curves in Fig. 6 show the FWHM of this peak as a function of coverage at RT and LT. The RT FWHM is above 2.3 eV at coverages as low as 0.06 Å, and reaches 3.0 eV at the highest coverage investigated. The LT FWHM, on the other hand, is only 1.6 eV up to 0.5 Å, then increases rapidly between 1 and 4 Å to reach the RT value. These results can be simply understood in terms of different growth mechanisms at RT and LT. At RT the surface mobility of Ag is quite large, and three-dimensional nucleation occurs very early on (see EELS results in subsection B). The density of nucleation sites is unknown, and so is, therefore, the statistical size of the clusters for a given coverage. However, an upper bound of 10^{12} cm^{-2} for the density of sites appears reasonable given that these nucleation sites are probably defects or steps generated during cleavage and that a higher density of charged defects would produce a large initial band bending. With this number, we can estimate that the average number of atoms per cluster reaches at least 40 at 0.05 ML coverage. Thus, a sizable fraction of the Ag atoms have a bulklike coordination at these coverages and the Ag-Ag interaction broadens the 4*d* band. The FWHM increases slowly as the band structure of the cluster develops into the full Ag band structure. At LT, on the other hand, the low-coverage overlayer consists of isolated Ag adatoms or very small clusters that produce the atomiclike 4*d* level and the small FWHM up to about 0.5 Å. Beyond this coverage, adatom proximity and coalescence

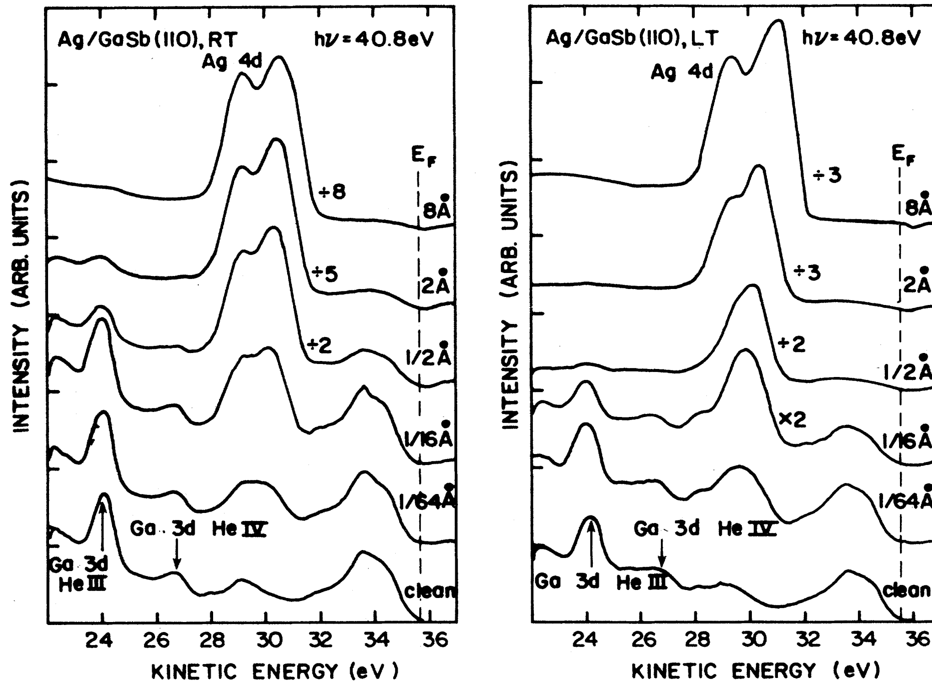

FIG. 5. Valence-band electron-distribution curve as a function of Ag deposition on the RT and LT GaSb surface.

of small clusters create a mostly bulklike environment and drastically increase the FWHM. Hybridization of the 4d and 5s levels takes place, as evidenced by the doublet resolved beyond 2 Å.

The dashed curves in Fig. 6 represent the FWHM for Ag/GaAs.[15] At low coverage they are ~0.4 eV above the Ag/GaSb curves. This difference is presumably due to two factors. First, the temperature reached in the present experiment is 35 K, as opposed to 80–90 K for Ag/GaAs. Second, the level of interface disruption by Ag is much larger on GaSb than on GaAs. Both effects contribute to an increase in the effective density of nucleation sites on GaSb, and therefore to a decrease in the statistical size of the clusters. For Ag on RT GaAs the FWHM reaches saturation around 2 Å, whereas it is not yet saturated at 8 Å for Ag on RT GaSb. Thus, the RT clusters are not as large on GaSb and might not become metallic as early as on GaAs.[15]

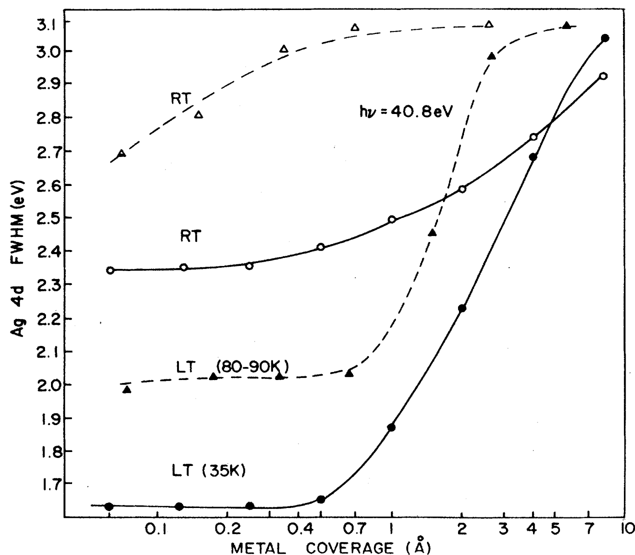

FIG. 6. Full width at half maximum of the Ag 4d band in Fig. 5 as a function of Ag coverage on RT and LT GaSb. The dashed curves correspond to Ag on GaAs(110) (Ref. 15).

Band-bending measurements were done on moderately and highly doped GaSb samples. The former were nondegenerate, except for the n type at LT. The latter were degenerate at RT and LT (Table I). Figures 7 and 8 show the E_F movements obtained from the shifts of the Ga 3d peak. For simplicity, the valence-band maximum (E_v) at RT and LT have been aligned. However, band-structure calculations have shown that the LT E_v should be about 50 meV below the RT E_v.[30] Two points should be made concerning these measurements. First, measurements on

TABLE I. Bulk position of the Fermi level with respect to the valence-band maximum at RT and LT. The GaSb band gap is 0.72 eV at RT and 0.81 eV at LT.

Doping (cm^{-3}) (at RT)	n 2.2×10^{17}	n 1.1×10^{18}	p 1.8×10^{17}	p 2.8×10^{18}
E_F-E_v (eV) at RT	0.71	0.77	0.07	−0.04
E_F-E_v (eV) at LT	0.84	0.91	0.01	−0.05

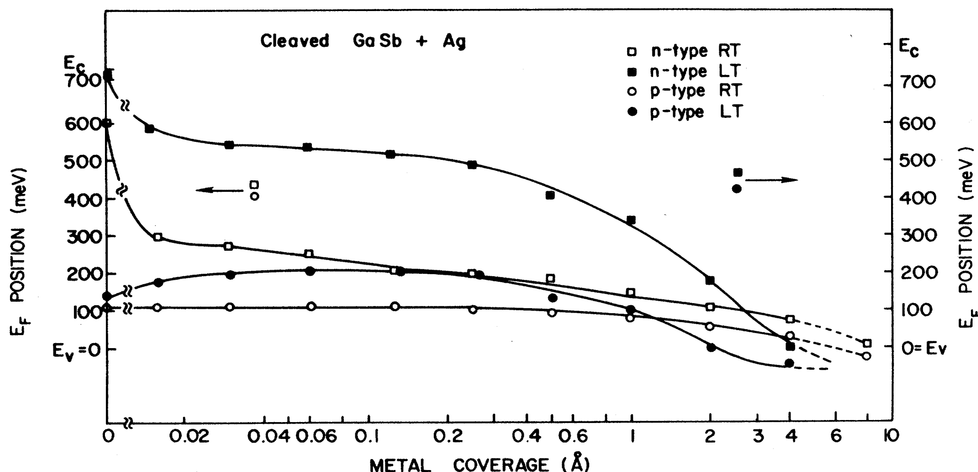

FIG. 7. Surface position of the Fermi level as a function of Ag coverage on the RT and LT moderately doped n- and p-type GaSb samples.

some n-type samples (mostly highly doped) show that the clean surface is affected by the He lamp: band bending increases just as a function of time, making the accurate assessment of the starting E_F position difficult. The uncertainty was somewhat reduced by making measurements on numerous moderately and highly doped n-type surfaces to provide sufficient statistics. The curves shown in Figs. 7 and 8 are the results of averaging between measurements done on several different surfaces. In addition, some measurements were performed by recording only the Ga $3d$ peak in order to minimize the time of exposure of the surface to the He lamp. Second, the large background in the EDC's at high Ag coverage, added to the attenuation of the Ga $3d$ signal, made the determination of the exact position of this peak beyond 4 Å coverage difficult. This problem is particularly acute at LT. The data corresponding to coverages of 4 Å and above are therefore presented by the dashed line to emphasize the underlying uncertainty.

Nonzero band bending is found on all cleaved surfaces: ~30–70 meV on p-type GaSb and ~50–150 meV on n-type GaSb. This band bending is inhomogeneous across the surface, and is presumably due to cleavage defects[31] or to perturbations by the He lamp (for n-type GaSb). Upon RT Ag deposition, E_F moves rapidly toward the valence band on n-type GaSb. On p-type GaSb, E_F moves very little below 0.5–1 Å, then moves down about 50–100 meV. Final pinning occurs about 50 meV below E_v, although the uncertainty in the Ga peak position above 4 Å makes the precise determination of this position difficult.

The differences between the RT and LT E_F movements are qualitatively similar to those found with most metals, particularly Ag on GaAs(110). On n-type GaSb, E_F moves down slower at LT than at RT below 0.5 Å, then drops to its final position near E_v. This is particularly clear on the moderately doped samples on which E_F moves down by 0.2 eV with 0.03 Å (similar to Ag/GaAs),

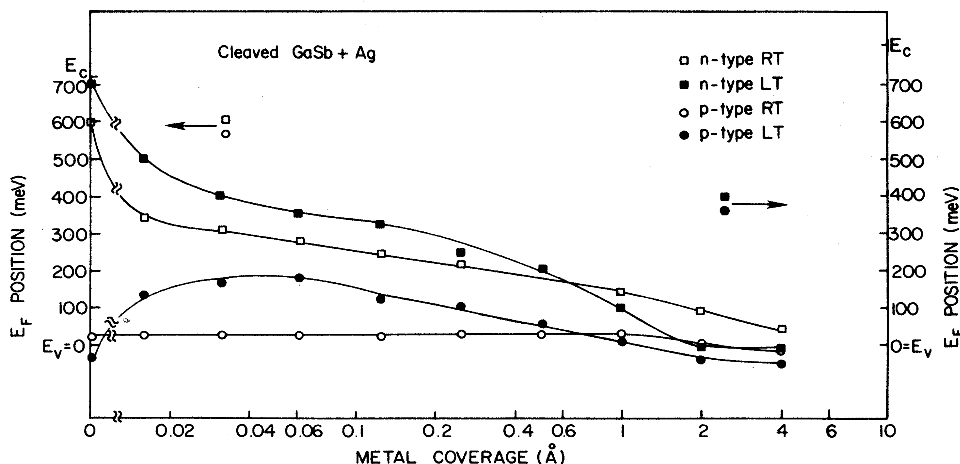

FIG. 8. Same as Fig. 7 for highly doped samples.

then remains approximately flat up to 0.5–1.0 Å. Poor cleavage (possibly due to strain in the bulk) and shifts due to exposure to the He lamp always produced a large initial band bending on the highly doped n-type samples. The slow down in E_F movement versus coverage is therefore not as clear as on the moderately doped n-type samples. On RT n-type samples, on the other hand, E_F moves down by about 0.4–0.5 eV at the same coverage, then slowly approaches the E_v when the coverage increases. On p-type samples, the LT E_F movement is characterized by an "overshoot" to a maximum position ~0.2 eV above E_v, followed by a movement toward its final pinning position.

We recalled in the Introduction that the differences between the RT and LT low-coverage band-bending data have been interpreted for GaAs(110) interfaces in terms of variations in overlayer morphology with temperature. The reduction in adatom surface mobility at LT produces overlayers consisting primarily of isolated atoms or very small clusters at low coverage, and homogeneous layers with little clustering at high coverage. The low-coverage GaSb band-bending results are therefore consistent with the model of donor states induced by the adsorption of isolated Ag atoms on surface atoms, presumably Ga (see EELS results in subsection B). These donor states are located 0.2–0.25 eV above E_v. These states pull E_F above E_v on the LT p-type surface, but do not affect E_F on n-type GaSb. The E_F rise is steeper on the highly doped than on the moderately doped samples because the donor level is fixed in the gap and the initital E_F position on the highly doped samples is lower with respect to E_v. Acceptor levels are in the upper part of the gap or above the con-duction-band minimum and, depending on their exact position, might produce the initial 0.2-eV drop of E_F. This initial drop may also result from surface effects induced by the uv lamp.

When the coverage on the LT surface increases, several effects come into play to modify the original adsorbate-induced states. First, the increasing number of polarized adatom-substrate bonds creates a dipole layer that electrostatically shifts the donor and acceptor levels.[13,14] The shift is toward E_v for bonds with charge transfer from the metal adatom to the substrate (weakly electronegative adatom). Second, a diversification of surface bonding sites is likely to occur with formation of Ag—Ga, Ag—Sb, as well as Ag—Ag bonds. Finally, the overlap of adatom wave functions takes place and leads to metallicity in the overlayer. These three factors contribute to a shift and broadening of the original donor and acceptor states, leading to additional E_F movement and, finally, pinning. The measurements indicate very clearly that the pronounced LT drop of E_F on n-type GaSb beyond 0.5 Å (Fig. 7) correlates with the abrupt increase in the Ag 4d bandwidth (Fig. 6). For Ag/GaAs, Stiles *et al.*[15] have shown that this increase is related to the onset of metallic character in the Ag layer, which occurs when the average cluster or island reaches a critical size [the order of magnitude is thought to be about 100 atoms (Ref. 32)]. We believe that the same criterion can be applied here.

This process is modified by clustering at RT. In particular, the adsorbate-induced states are modified by adatom interaction. In general terms, the energy difference between donor and acceptor levels is reduced[12,13] and the levels are broadened by the overlap of adatom wave functions at much smaller coverages than at LT. The E_F overshoot seen at LT is by-passed because the overlayer never consists of isolated adatoms. In the limit of large clusters, these levels become part of a quasicontinuum of (metallic) states. Thus, local band bending underneath and around the clusters corresponds to pinning by a metal rather than by discrete adsorption-induced states.

Both RT and LT final E_F positions are found at or below E_v. Although these are difficult to establish precisely for reasons mentioned above, we are confident that E_F is not pinned more than 30–50 meV above E_v. This is incompatible with the position inferred from I-V measurements on thick Ag/(n-type GaSb) diodes by Walters *et al.*[22] They find a barrier height of 0.33–0.35 eV for vacuum-cleaved surfaces which, given the 0.72-eV band gap, places E_F at about midgap. However, the ideality factors of these diodes were consistently equal to or larger than 2, casting serious doubts on the determination of the exact barrier height. Better ideality factors of the order of 1.2 were obtained for Al on molecular-beam-epitaxy (MBE) -grown GaSb(100) by Poole *et al.*,[33] indicating that the quality of the bulk material might be in question for the ideality of the dipole. They also found higher barriers (~0.55 eV) than for Al on vacuum-cleaved GaSb (0.39–0.40 eV, $n=2$). The 0.55-eV barriers correspond to E_F 0.17 eV above E_v. The final E_F position found in the present work is very close to that found by Chye *et al.* for Au/(n-type GaSb) with photoemission spectroscopy.[21] Pinning at E_v was attributed in this case to metal-induced defects. This position, however, is also very close to the charge-neutrality level at 70 meV above E_v, as calculated by Tersoff.[23] Given the simplicity of the theoretical model and the uncertainty of our measurements, we conclude that the observed pinning position is not incompatible with Tersoff's prediction.

Defects are present at the Ag/GaSb interface, if only as a result of the interface dissociation illustrated by the AES or photoemission results presented above or by Walters *et al.*,[22] and the density of defects is presumably smaller at LT than at RT. Thus, the low-coverage part of the E_F movement on p-type GaSb cannot be explained with defects. In particular, if defects are responsible for the LT overshoot, a different kind of defect would have to be involved at RT. We will assume that this is not the case, although no formal proof can be given at this point. Furthermore, defects are expected to appear in sizable density at coverages far below those where final E_F pinning occurs. The critical thickness of 2–4 Å at which final pinning occurs is about the same for all the metals deposited on LT GaAs, regardless of interface reactivity. We believe that it relates much more directly to the coverage necessary to complete the first layer or two of the overlayer, thus bringing adatoms in close proximity and delocalizing the gap states, than to the eventual formation of interface defects. We cannot rule out the role of defects in modulating the final E_F positions, but they do

not appear to play the dominant role in the pinning process.

IV. CONCLUSIONS

In conclusion, we have confirmed that overlayer morphology plays a fundamental role in the initial stages of surface band bending and that the trend in E_F movements observed with interfaces formed on LT GaAs also applies to GaSb. Our low-coverage band-bending results are well explained with a model of Ag-induced gap states, which involves a donor level 0.2–0.25 eV above E_v. The acceptor level is near or above the conduction-band minimum. As the overlayer grows, these states are shifted down by the overlayer-substrate dipole effect and broaden into bands. E_F pinning is slightly below E_v and correlates with the onset of metallicity in the overlayer.

ACKNOWLEDGMENTS

We would like to thank Dr. A. Gouskov for providing the GaSb ingots, Dr. L. Gouskov for performing Hall-effect and bulk E_F-position measurements, and Mrs. V. Coronato for technical assistance. This work was supported by a grant from the U.S. National Science Foundation (No. DMR-87-09531). Partial support was also provided by the General Motors Corporation. The Laboratoire d'Etudes des Surfaces, Interfaces et Composants, is "unité associeé du Centre National de la Recherche Scientifique No. D07870."

[1] M. K. Kelly, A. Kahn, N. Tache, and G. Margaritondo, Solid State Commun. **58**, 429 (1986).
[2] K. Stiles, A. Kahn, D. G. Kilday, and G. Margaritondo, J. Vac. Sci. Technol. B **5**, 987 (1987).
[3] K. Stiles, S. F. Horng, A. Kahn, J. McKinley, D. G. Kilday, and G. Margaritondo, J. Vac. Sci. Technol. B **6**, 1392 (1988).
[4] K. Stiles, A. Kahn, D. G. Kilday, J. McKinley, and G. Margaritondo, J. Vac. Sci. Technol. A **6**, 1462 (1988).
[5] K. Stiles, A. Kahn, D. G. Kilday, and G. Margaritondo, J. Vac. Sci. Technol. A **6**, 1511 (1988).
[6] R. Cao, K. Miyano, T. Kendelewicz, K. K. Chin, I. Lindau, and W. E. Spicer, J. Vac. Sci. Technol. B **5**, 998 (1987).
[7] R. Cao, K. Miyano, T. Kendelewicz, I. Lindau, and W. E. Spicer, J. Vac. Sci. Technol. A **6**, 1571 (1988).
[8] C. M. Aldao, I. M. Vitomirov, G. D. Waddill, and J. H. Weaver, Appl. Phys. Lett. **53**, 2647 (1988).
[9] G. D. Waddill, C. M. Aldao, I. M. Vitomirov, and J. H. Weaver, in Proceedings of the 16th International Conference on the Physics and Chemistry of Semiconductor Interfaces [J. Vac. Sci. Technol. (to be published)].
[10] W. Mönch, J. Vac. Sci. Technol. B **6**, 1270 (1988).
[11] A. Kahn, K. Stiles, D. Mao, S. F. Horng, K. Young, J. McKinley, D. G. Kilday, and C. Margaritondo, J. Electron Mater. **18**, 33 (1989).
[12] A. Kahn, K. Stiles, D. Mao, S. F. Horng, K. Young, J. McKinley, D. G. Kilday, and G. Margaritondo, in *Proceedings of the NATO Advanced Study Institute Workshop, Garching, 1988*, edited by I. Batra (Plenum, New York, 1989).
[13] J. E. Klepeis and W. A. Harrison, in Ref. 9.
[14] I. Lefebvre, M. Lannoo, and G. Allan, Phys. Rev. B **39**, 13 518 (1989).
[15] K. Stiles and A. Kahn, Phys. Rev. Lett. **60**, 440 (1988).
[16] D. Mao, K. Young, K. Stiles, and A. Kahn, J. Appl. Phys. **64**, 4777 (1988).
[17] M. Prietsch, M. Domke, C. Laubschat, T. Mandel, C. Xue, and G. Kaindl, Z. Phys. B **74**, 21 (1989).
[18] M. Prietsch, M. Domke, C. Laubschat, and G. Kaindl, Phys. Rev. Lett. **60**, 436 (1988).
[19] R. Cao, K. Miyano, I. Lindau, and W. E. Spicer, J. Vac. Sci. Technol. A **7**, 861 (1989).
[20] R. E. Vitturo, J. L. Shaw, C. Mailhiot, L. J. Brillson, N. Tache, J. McKinley, G. Margaritondo, J. M. Woodall, P. D. Kirchner, G. D. Pettit, and S. L. Wright, Appl. Phys. Lett. **52**, 2052 (1988).
[21] P. W. Chye, I. Lindau, P. Pianetta, C. M. Garner, C. Y. Su, and W. E. Spicer, Phys. Rev. B **18**, 5545 (1978).
[22] S. A. Walters and R. H. Williams, J. Vac. Sci. Technol. B **6**, 1421 (1988).
[23] J. Tersoff, Phys. Rev. B **30**, 4874 (1984).
[24] D. Mao, L. Soonckindt, A. Kahn, A. Terrasi, Y. Hwu, and G. Margaritondo, J. Vac. Sci. Technol. (to be published).
[25] J. van Laar, A. Huijser, and T. L. van Rooy, J. Vac. Sci. Technol. **14**, 894 (1977).
[26] C. R. Bonapace, D. W. Tu, K. Li, and A. Kahn, J. Vac. Sci. Technol. B **3**, 1099 (1985).
[27] C. R. Bonapace, K. Li, and A. Kahn, J. Phys. (Paris) Colloq. **45**, C5-409 (1984).
[28] K. Stevens, L. Soonckindt, and A. Kahn (unpublished).
[29] R. M. Feenstra, C. K. Shih, and P. Mårtensson, in Ref. 9.
[30] L. Soonckindt, J. Bonnet, P. Masri, and L. Lassabatere, Surf. Sci. **130**, L337 (1983).
[31] J. Bonnet, L. Soonckindt, A. Ismail, and L. Lassabatere, Thin Solid Films **151**, 103 (1987).
[32] G. K. Wertheim, S. B. DiCenzo, and D. N. E. Buchanan, Phys. Rev. B **33**, 5384 (1986).
[33] I. Poole, M. E. Lee, M. Missous, and K. E. Singer, J. Appl. Phys. **62**, 3988 (1987).